

RESULTS OF APL RAIN GAUGE NETWORK MEASUREMENTS IN MID-ATLANTIC
COAST REGION AND COMPARISONS OF DISTRIBUTIONS WITH CCIR MODELS

Julius Goldhirsh, Norman Gebo, and John Rowland

Applied Physics Laboratory, The Johns Hopkins University
Laurel, Maryland, 20707-6099

Abstract

In this effort are described cumulative rain rate distributions for a network of nine tipping bucket rain gauge systems located in the mid-Atlantic coast region in the vicinity of the NASA Wallops Flight Facility, Wallops Island, Virginia. The rain gauges are situated within a gridded region of dimensions 47 km east-west by 70 km north-south. Distributions are presented for the individual site measurements and the network average for the year period June 1, 1986 through May 31, 1987. A previous six year average distribution derived from measurements at one of the site locations is also presented. Comparisons are given of the network average, the CCIR climatic zone, and the CCIR functional model distributions, the latter of which approximates a log normal at the lower rain rate and a gamma function at the higher rates.

1.0 Introduction

Earth-satellite telecommunications may be seriously degraded by rain attenuation at frequencies above 10 GHz. In order to account for realistic fade margins, design engineers require information as to the expected number of hours per year given fade levels are exceeded. This information can be derived employing direct attenuation measurements, or it may be inferred from rain attenuation models using rain rate statistics of the type described in this effort [CCIR, 1986].

We address here the following specific questions for the mid-Atlantic Coast region: (1) What are the variabilities in rain rate statistics due to microclimate effects? (2) How do short term spatially averaged rain distributions compare with longer term temporally averaged statistics? (3) What are appropriate functional forms for describing rain rate distributions? (4) How does the network rain rate distribution compare with the CCIR model distributions? A comprehensive description of this effort is described by Goldhirsh et al [1988].

2.0 Experimental Aspects

The gauges employed are of the tipping bucket type and are calibrated such that with each 0.25 mm of rainfall, a bucket tip occurs resulting in a 100 millisecond switch closure interval. Each rain gauge is connected to a Commodore 64 computer. The time of each bucket tip is stored within the computer to a 1 millisecond resolution. The individual tipping times are transferred from computer memory and recorded on a 5-1/4 inch floppy disk at two hour intervals. Also recorded are such items as file number, Julian Day, time the file written to disk, and total rainfall in mm.

Ten rain gauges of the type described above were located within a radial range of 60 km from the SPANDAR facility. The site locations (labeled #1 - #10) are depicted in the map of Figure 1. Only the results of nine gauges are reported here because of the close proximity of two of them (Sites #4 and #5). The individual rain gauge systems are located at the home grounds of staff working at the NASA Wallops Flight Facility. The staff calibrates and maintains these systems on a continual basis. Calibrations are performed at least several times per week. The floppy disks are removed on a weekly basis for subsequent reduction and analysis.

3.0 Cumulative Distributions of Rain Rate

3.1 Spatial Variability of Rain Rate Distributions

In Figure 2 is shown a composite of individual rain rate distributions for each of nine sites. The vertical scale represents the percentage of the year the abscissa value of the rain rate is exceeded. Each curve is labeled with the corresponding site number both at the higher and lower percentage values. Since the rain rate statistics below .001% of the year (5.25 minutes) are noted to be noisy, we characterize the results only down to this percentage level. We observe that at the .001% level the rain rates vary between 85 mm/hr (Site #6) and 125 mm/hr (Site #10). The distance between these sites is only 15 km. This relatively large variation (47% change relative to the smaller value) in the statistics for such a short separation is attributed to the micro-climate effects caused by Site #6 being located closer to the ocean (on Chincoteague Island). The ocean has a tendency to dampen the more intense convective rain rates which originate over land and are sustained by ground heating, as for example, air mass type showers. At the 0.1% level (8.8 hours), the rain rates vary between 15 mm/hr (Site #9) and 25 mm/hr (Site #2), a 67% increase relative to the smaller value. The distance between these sites are noted to be approximately 57 km.

3.2 Network Average Cumulative Rain Rate Distribution

In Figure 3 is presented the combined average network rain rate distribution (circled data points). These were obtained by averaging the percentages at each rain rate level. We note the statistical noise in the vicinity of the .001% range is mitigated significantly as compared to the distributions for individual sites. This is attributed to the statistical smoothing in the averaging process. Also plotted is the 6 year average cumulative rain rate distribution measured at the SPANDAR location (Site #10) during the period 1977-1983 [Goldhirsh, 1983a; 1983b]. This distribution was taken only up to 100 mm/hr since the smallest clock time resolution for these previous measurements was one second resulting in discernible quantization uncertainties at the higher rain rates. It is interesting to note that the network average and the time average distributions practically overlap. It has yet to be established whether it is fortuitous that the spatial average of distributions is equivalent to the long term temporal average for the region under investigation as suggested by the results.

3.3 Best Fit Rain Rate Distributions

It has been suggested that the rain rate distribution can be represented by a log normal functional form in the approximate interval 2 - 50 mm/hr although the rain rate interval of validity is dependent on the climatic region [CCIR, 1986]. Segal [1980], employing measurements made in Canada, demonstrated that a power law relationship satisfactorily approximates the entire cumulative rain rate distribution for rain rates exceeding 5 mm/hr. More recent analysis suggests that rain rate distribution may be also approximated by the log-normal distribution for the lower rain rates and a gamma distribution at the higher rates [Moupfouma, 1985].

3.3.1 Log Normal Distribution

In Figure 4 is shown the average rain rate distribution for the rain gauge network (circled points) plotted vis a vis a Gaussian ordinate (percentage) and a logarithmic abscissa (rain rate). A log normal distribution for this representation is indicated by points which lie along a straight line. We note that the data points (circled points) practically overlap with the fitted log normal distribution (straight solid line) in the rain rate interval 3 to 40 mm/hr. Thereafter, the data points deviate considerably from the log normal. This deviation is considered real as it is consistent with previous multi-year rain gauge measurements made at Wallops Island, Virginia (Figure 3) [Goldhirsh, 1983]. The distribution is consistent with

$$M = \langle \log_{10} R \rangle = -1.725 \quad (1)$$

$$\sigma^2 = \langle (\log_{10} R - M)^2 \rangle = 0.912 \quad (2)$$

where M and σ are the mean and standard deviation of $\log_{10} R$, respectively, associated with the log normal.

3.3.2 Power Distribution

Although the log normal distribution has physical ramifications as pointed out by Lin [1975], it represents an awkward functional form for computational purposes. For this reason, we examine here other more convenient functional representations. In Figure 5 is plotted the network rain rate distribution in the 3 to 30 mm/hr interval and the associated least squares power fit. This is given by

$$P\{ r > R \} = A R^{-B} \quad (3)$$

where

$$A = 6.132 \quad (4)$$

$$B = -1.469 \quad (5)$$

and where (3) is directly given in terms of percentage. We note that the power curve fit in Figure 5 agrees with the rain rate values to within a small fraction of 1 mm/hr for any given percentage within the interval 3 to 30 mm/hr. It has a functional form which is significantly easier to handle computationally than the log normal.

3.3.3 Exponential Fit

In Figure 6 is plotted the network distribution in the rain rate interval 30 to 140 mm/hr. Also plotted is the least square exponential (solid line) given by the form

$$P(r > R) = \alpha \exp[- \beta R] \quad (6)$$

where

$$\alpha = 0.1488 \quad (7)$$

$$\beta = 0.04615 \quad (8)$$

and where (6) is also expressed in terms of percentage. The exponential fit describes the rain rate distribution over the higher rain rate interval (30 - 140 mm/hr) with excellent accuracy. At 140 mm/hr we observe only a maximum error of less than 3% in rain rate.

4.0 Comparison with CCIR Model Distributions

We examine here two rain rate distribution models which have been suggested by the CCIR (1986) for use with earth-satellite and terrestrial rain attenuation predictions.

4.1 Climatic Zone Distributions

The climatic zone model divides the world into 14 climatic regions notated A through P (Figure 7). Each zone has associated with it a unique rain rate distribution based on averages of measured distributions. The general location of the rain gauge network (circled area) is in climatic zone K along the mid-Atlantic coast in proximity to region M. The rain rate distributions for the rain gauge network and for regions E, F, K, and M are given in Figure 8. We note that the mid-Atlantic coast network distribution lies between those for regions M and K. This is consistent with the fact the network lies in region K but close to M. Since an abrupt change in the rain rate distribution is obviously non-physical at the region borders, one should expect the network distribution to lie between the distributions for the two climatic zones as indicated.

4.2 Distribution Based On .01% Rain Rate

A model distribution has been proposed by Moupfouma [1985] which approximates a log-normal function at the lower rain rates and a gamma function at the higher rain rates [CCIR, 1986]. This model function is given by

$$P(r > R) = \frac{a \exp(- u R)}{R^b} \quad (9)$$

where

$$a = 10^{-4} (R_{.01})^b \exp(u R_{.01}) \quad (10)$$

$$b = 8.22 (R_{.01})^{-.584} \quad (11)$$

The probability (9) should be multiplied by 100 for conversion to percentage, and $R_{.01}$ represents the measured rain rate at the .01 percent probability. Equating $R_{.01} = 58$ mm/hr (the rain gauge network rain rate at the .01% level), the corresponding rain rate distribution was calculated and plotted in Figure 9. Also shown plotted is the measured rain gauge network distribution. The model rain rate distribution is noted to overestimate the rain rate by approximately 18% at the .001% probability (107 versus 126 mm/hr), and underestimate the rain rate by 21% at the .1% probability (16.5 versus 13.1 mm/hr).

5.0 Conclusions

The results of the network measurements demonstrate that an extreme range of rain rate statistics may exist over short distance intervals; especially near coastal areas. One means in which to smooth out these statistics is to average the distributions for a network of such measurements. Previous multi-year averaging of individual rain rate statistics has been found to have similar smoothing effects and result in a distribution which agreed closely with the short term network average.

In characterizing rain rate statistics in the above described mid-Atlantic coast region, it is suggested that the cumulative distributions be described with a power curve fit at the smaller rain rate interval (3 - 30 mm/hr) and with an exponential fit at the larger rain rates (30 - 140 mm/hr). The log normal distribution provides a good fit over the smaller interval, but is difficult to use computationally. The CCIR model distribution of Moupfouma [1985] is adequate if a 20% rain rate error is acceptable.

6.0 Acknowledgements

The authors are grateful to those individuals in whose homes the rain gauges were located and cared for. In alphabetical order the names are as follows: Lester Atkinson, Albert Barnes, Norris Beasley, Martin Eby, Charles Ethridge, Norman Gebo, Steve Jones, Eugene Ward, and Sam West. The authors are also grateful to Karen Melvin for typing this manuscript. This work was supported jointly by NASA Headquarters, Communications Division, and NASA Goddard Space Flight Center under Contract N00039-87-C-5301.

7.0 References

- CCIR (International Radio Consultative Committee), "Recommendations and Reports of the CCIR, 1986", XVith Plenary Assembly, 5, Dubrovnik (Propagation in Non-Ionized Media), 1986.
- Goldhirsh, J., N. E. Gebo, and J. R. Rowland, "Rain Rate Statistics From A Rain Gauge Network in a Mid-Atlantic Coast Region", JHU/APL Technical Report, S1R88U--014, April 1988.

Goldhirsh, J., "Yearly Variations of Rain-Rate Statistics at Wallops Island and Their Impact on Modeled Slant Path Attenuation Distributions", IEEE Trans. on Antennas & Propagation, AP-32, No. 6, pp. 918-921, November, 1983.

Goldhirsh, J., "Yearly and Monthly Rain Rate Statistics at Wallops Island, Virginia Over a Six Year Period", JHU/APL Technical Report S1R83U-039, December, 1983 (Johns Hopkins University/Applied Physics Laboratory, Johns Hopkins Road, Laurel, Maryland 20707).

Lin, S.H., "A Method for Calculating Rain Attenuation Distribution on Microwave Paths", Bell System Technical Journal, 54, July-August, 1975.

Moupfouma, F., "Model of Rainfall Rate Distribution for Radio System Design," IEE Proc., Vol 132, Pt H, 1, pp. 39-43, Feb. 1985.

Segal, B., "An Analytical Examination of Mathematic Models for the Rainfall Rate Distribution Function," Ann. des. Telecomm., Vol 35, pp. 434-438, 1980.

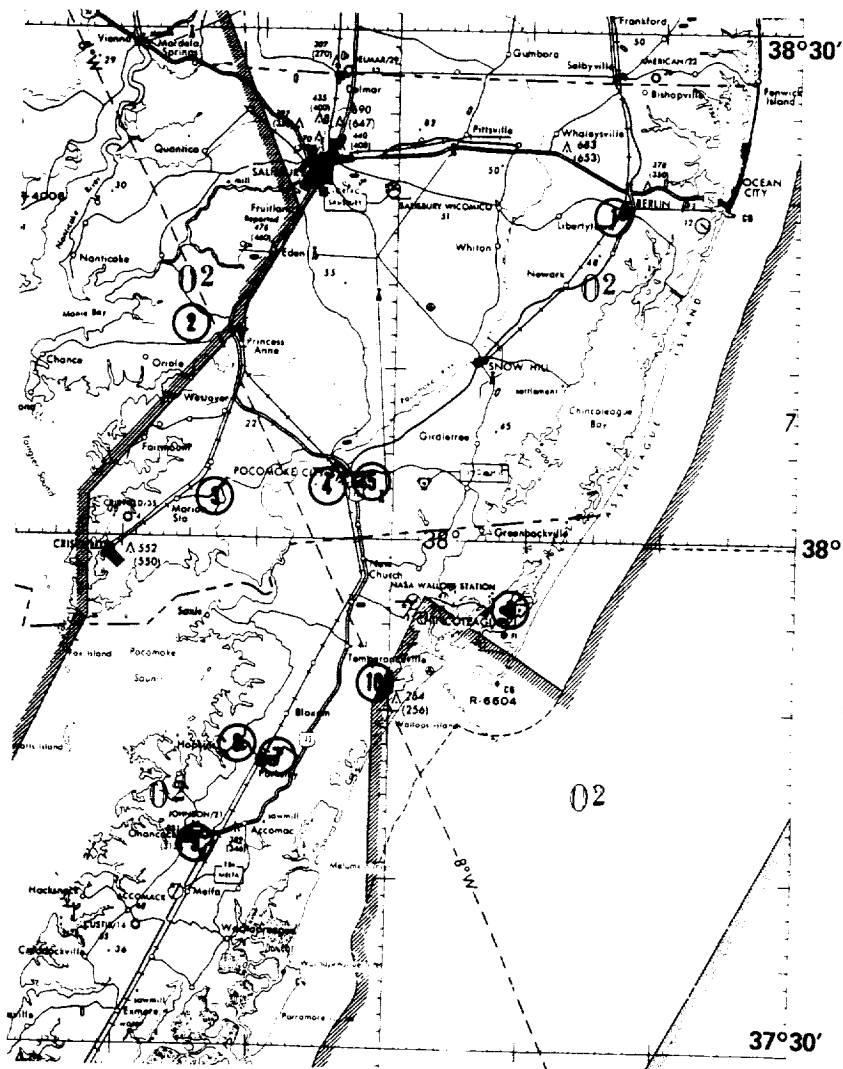


Figure 1 Map showing rain gauge site locations in vicinity of Wallops Island, Virginia

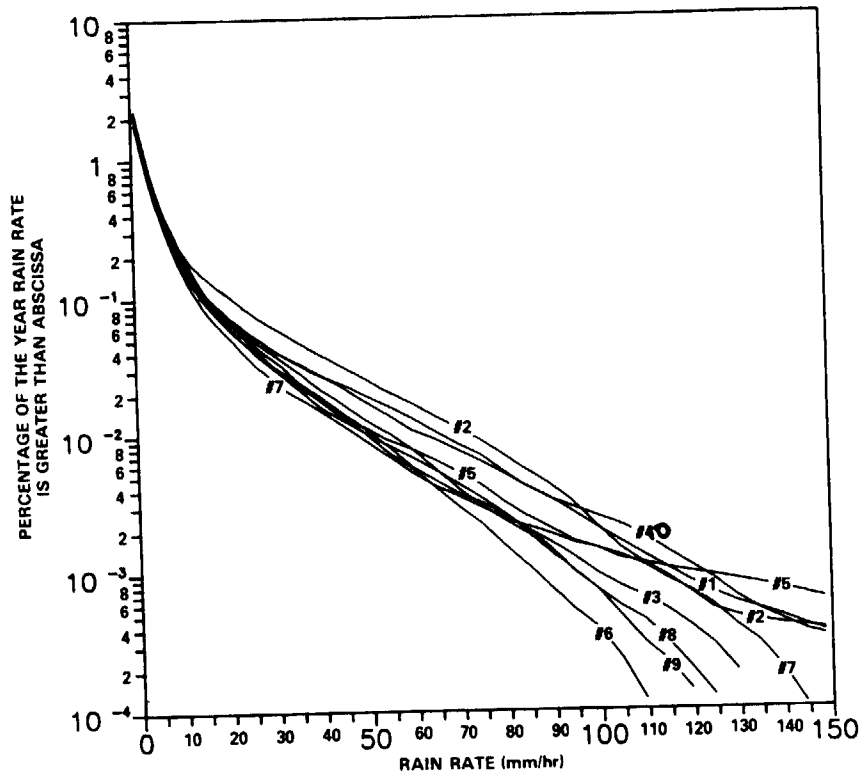


Figure 2 Composite of yearly cumulative rain rate distributions for each of nine site locations in vicinity of Wallops Island, Virginia (June 1986 - May 1987)

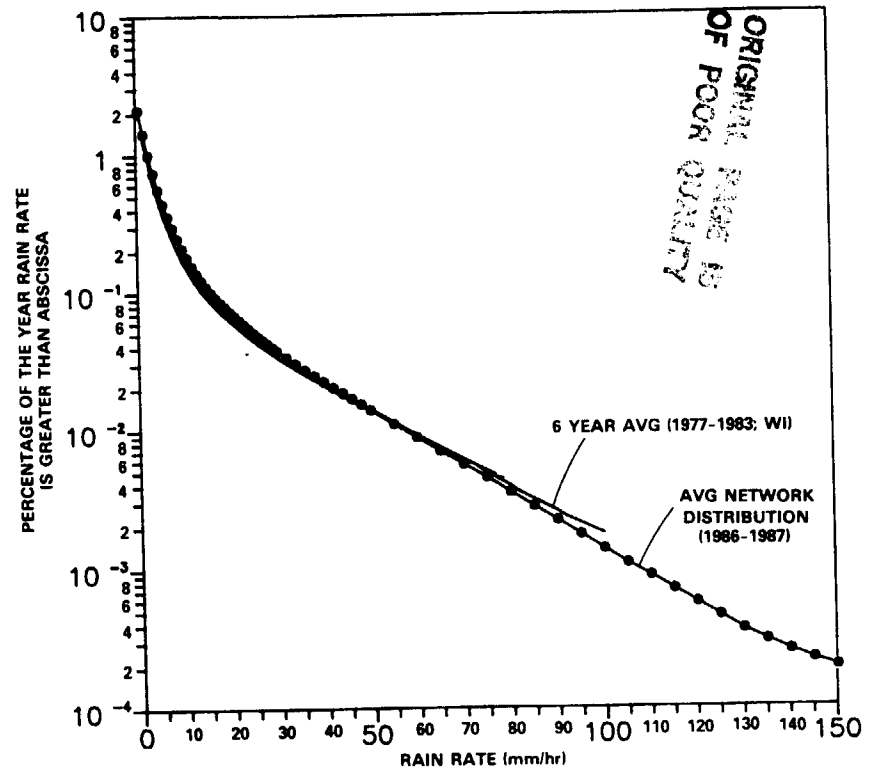


Figure 3 Combined average network yearly cumulative rain rate distribution (June 1986 - May 1987) and comparison with previous 6 year average rain rate distribution at Wallops Island, Virginia

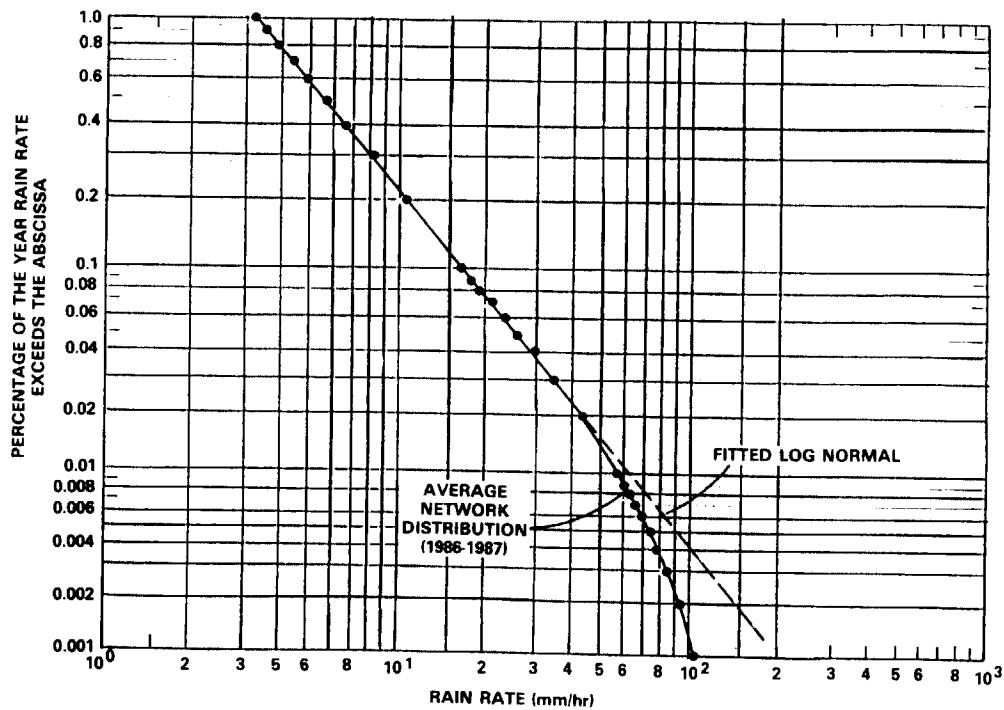


Figure 4 Combined average cumulative rain rate distribution for 12 month period and corresponding log normal fit (solid line).

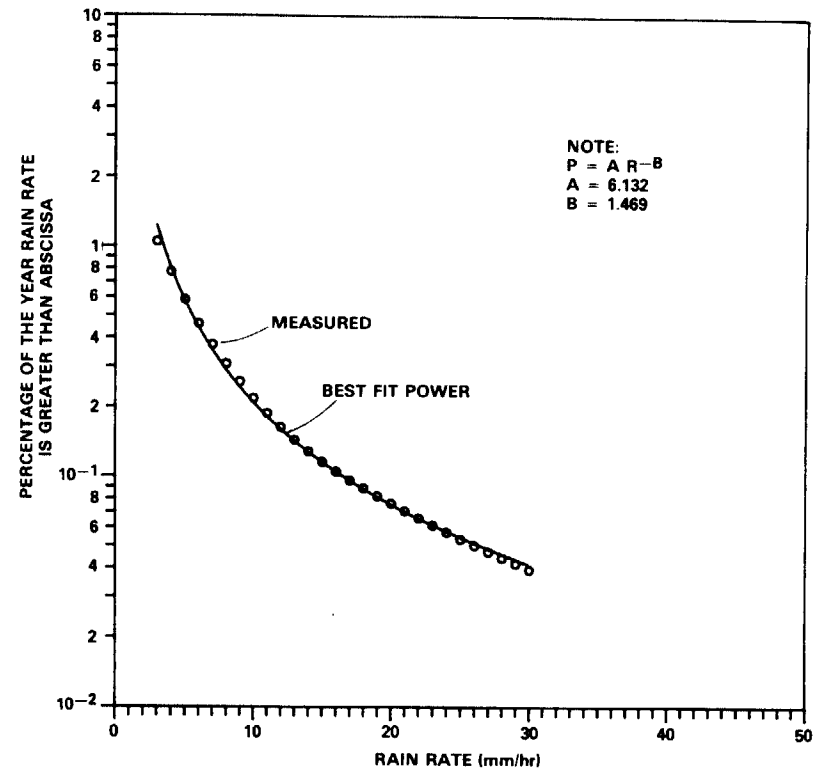


Figure 5 Average network yearly cumulative rain rate distribution and best fit power distribution (3-30 mm/hr).

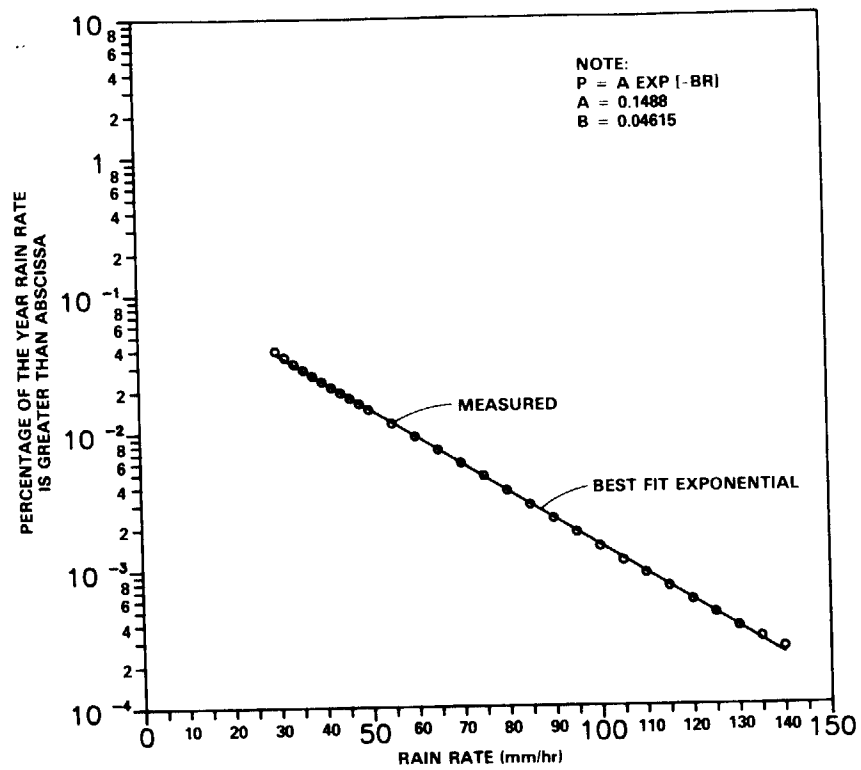


Figure 6 Average network yearly cumulative rain rate distribution and best fit exponential (30-140 mm/hr)

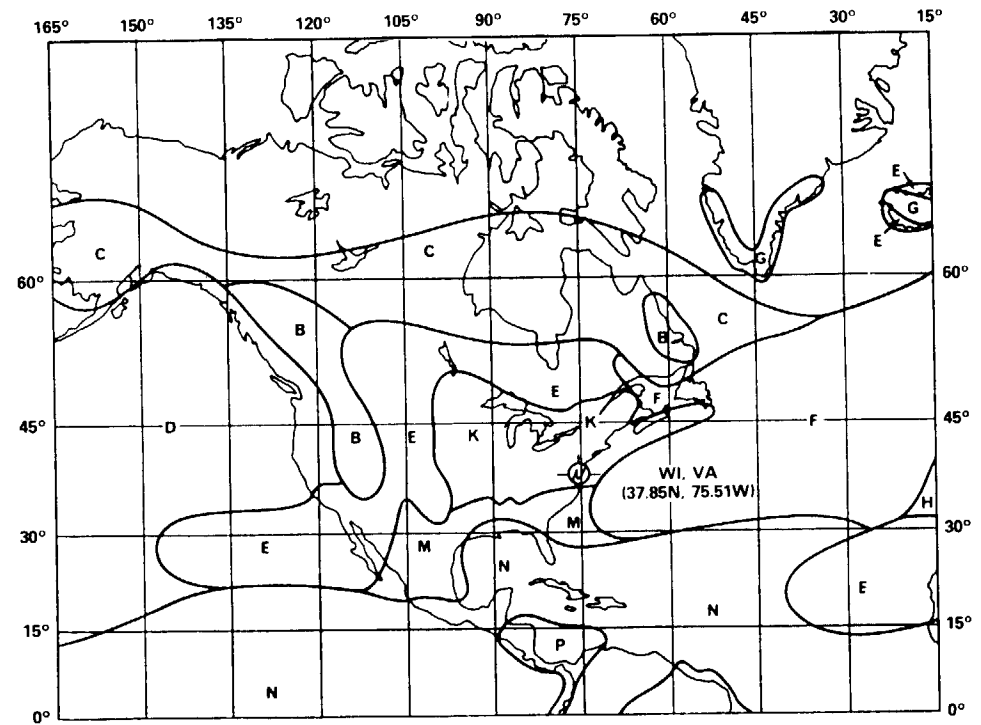


Figure 7 Map showing CCIR climatic zones with designated rain rate distributions (CCIR Report 563-3).

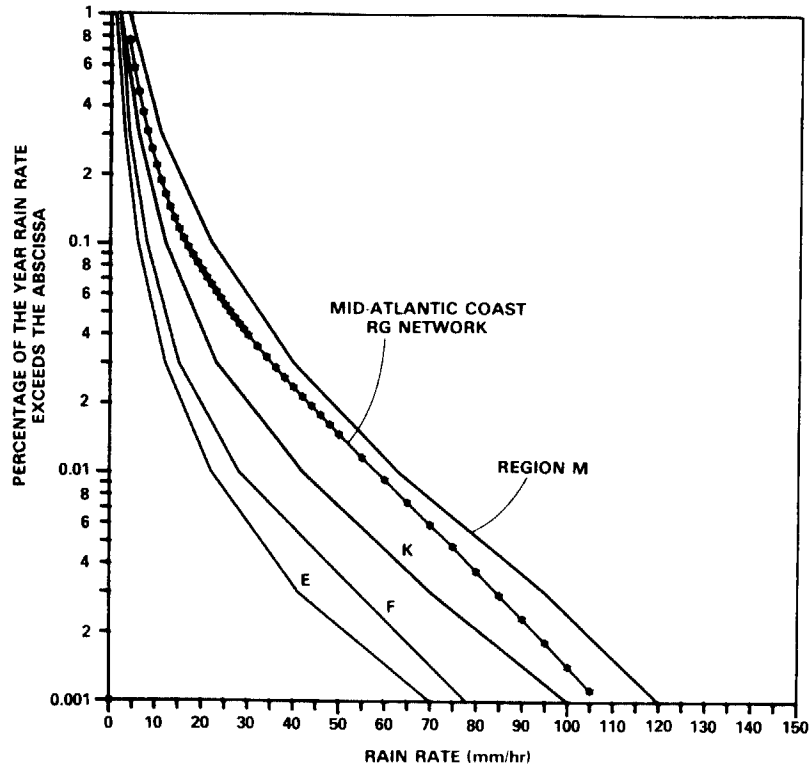


Figure 8 Comparison of rain gauge network rain rate distribution for mid-Atlantic coast and CCIR climatic zone rain rate distributions (CCIR Report 563-3).

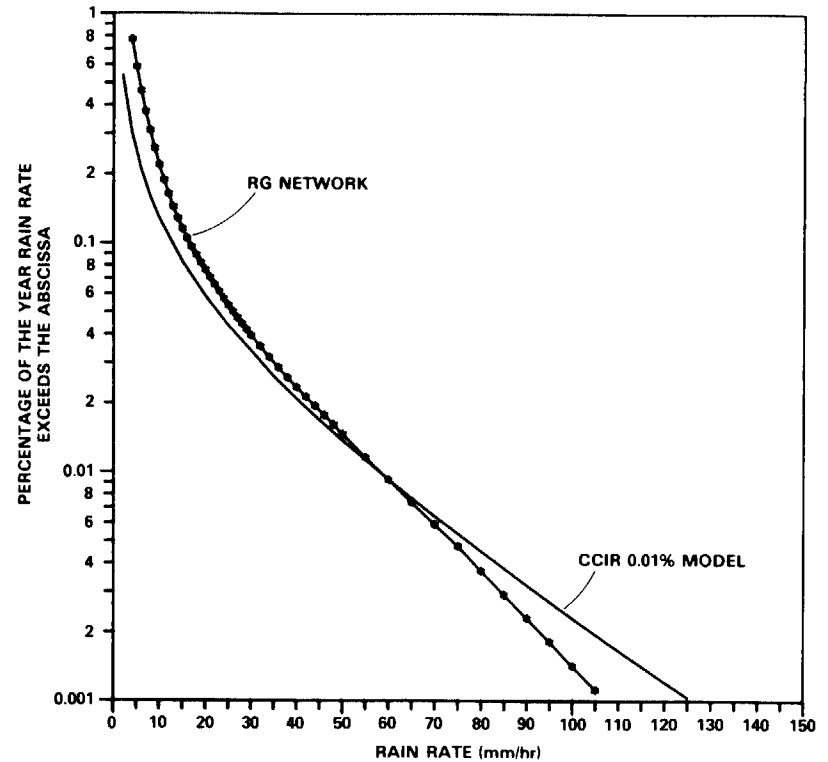


Figure 9 Comparison of rain rate distribution for mid-Atlantic coast rain gauge network and CCIR model distribution based on .01% rain rate (CCIR Report 563-3).